Biophysical Journal Volume 73 November 1997 2742–2751

Dynamic Properties of Monomeric Insect Erythrocruorin III from *Chironomus thummi-thummi*: Relationships between Structural Flexibility and Functional Complexity

Ernesto E. Di Iorio, Ivano Tavernelli, and Weiming Yu
Laboratorium für Biochemie I, ETH Zurich, 8092 Zurich, Switzerland

ABSTRACT We have investigated the kinetics of geminate carbon monoxide binding to the monomeric component III of *Chironomus thummi-thummi* erythrocruorin, a protein that undergoes pH-induced conformational changes linked to a pronounced Bohr effect. Measurements were performed from cryogenic temperatures to room temperature in 75% glycerol and either 0.1 M potassium phosphate (pH 7) or 0.1 potassium borate (pH 9) after nanosecond laser photolysis. The distributions of the low temperature activation enthalpy $g(H)$ for geminate ligand binding derived from the kinetic traces are quite narrow and are influenced by temperature both below and above ~170 K, the glass transition temperature. The thermal evolution of the CO binding kinetics between ~50 K and ~170 K indicates the presence of some degree of structural relaxation, even in this temperature range. Above ~220 K the width of the $g(H)$ progressively decreases, and at 280 K geminate CO binding becomes exponential in time. Based on a comparison with analogous investigations of the homodimeric hemoglobin from *Scapharca inaequivalvis*, we propose a link between dynamic properties and functional complexity.

INTRODUCTION

Ferrous heme proteins form photolabile complexes with ligands, a property that renders flash photolysis particularly suited to study their binding kinetics (Antonini and Brunori, 1971). The availability of pulsed lasers as photolyzing sources and of cryogenic devices has enormously expanded the time and temperature ranges that can be explored by flash photolysis, such that this experimental approach has become one of the most valuable tools for investigating protein dynamics and their functional implications. After the pioneering work of the Frauenfelder group (Austin et al., 1973), laser flash photolysis over broad temperature ranges has been extensively used to perform investigations along three major lines. On one side, the dynamic properties of sperm whale myoglobin (SW-Mb), taken as a model system, have been investigated in great detail, also using several engineered mutants of this protein. Among many fundamental findings, the work done on SW-Mb has allowed the detection of different tiers of conformational transitions (Ansari et al., 1985). In some cases spectroscopic markers for the substates within a single tier have been identified, and their interconversion has been followed experimentally (Abadan et al., 1995; Ansari et al., 1987; Bosenbeck et al., 1992; Braunstein et al., 1993; Causgrove and Dyer, 1993; Frauenfelder et al., 1990; Gilch et al., 1993; Hong et al., 1990; Ivanov et al., 1994; Johnson et al., 1996). Next, a comparative analysis on structurally and functionally unrelated heme proteins, such as leghemoglobin (Stetzkowski et al., 1985), horseradish peroxidase (Doster et al., 1987), rat liver cytochrome p-450 (Richter and Di Iorio, 1991), and lignin peroxidase (Glumoff, 1991) has been performed. Even though different in the details, the same overall kinetic features, briefly outlined in the following paragraph, have been observed over broad temperature ranges in all systems investigated. Finally, comparative studies on heme proteins with highly homologous folding, but differing in their functional properties, have provided insights into the relationships between structure-dynamics and function (Alberding et al., 1978; Bisig et al., 1995; Boffi et al., 1994; Cupane et al., 1993; Di Iorio et al., 1991, 1993; Dlott et al., 1983). The use of experimental approaches other than flash photolysis, such as inelastic neutron scattering (Andreani et al., 1995; Doster et al., 1989, 1990), light absorption spectroscopy (Cupane et al., 1994; Di Pace et al., 1992; Schomacker and Champion, 1986; Srajer and Champion, 1991), Raman spectroscopy (Friedman et al., 1982, 1990; Morikis et al., 1989, 1990; Schweitzer-Stenner et al., 1992; Spiro, 1988), Mössbauer spectroscopy (Parak, 1989; Prusakov et al., 1995), and Rayleigh scattering of Mössbauer radiation (Krupyanskii et al., 1990), extended to several macromolecular systems, have proved the general validity of the information on protein dynamics derived from flash photolysis on heme proteins.

Rebinding of a ligand to a heme protein after photolysis can be generally described in terms of a three-well reaction scheme:

$$A \Leftarrow B \Leftrightarrow S \qquad (1)$$

where A denotes the ligand bound state, and B and S refer, respectively, to the dissociated states, with the photolyzed ligand trapped in the vicinity of the heme or free to migrate in the surrounding solvent. Below ~160 K photolysis leads

Received for publication 7 March 1997 and in final form 19 August 1997.

Address reprint requests to Laboratorium für Biochemie I, ETH Zurich, Universitätstrasse 16, 8092 Zurich, Switzerland. Tel.: 41-1-632-3137; Fax: 41-1-632-1121; E-mail: diiorio@bc.biol.ethz.ch.

Dr. Yu's present address is Laboratory of Fluorescence and Dynamics, Department of Physics, University of Illinois at Urbana-Champaign, 1110 West Green Street, Urbana, IL 61801-3080.

0006-3495/97/11/2742/10 $2.00

only to the B state, and the recombination process, referred to as geminate rebinding, is nonexponential in time. This behavior is attributed to the freezing of large-scale structural fluctuations occurring at high temperatures such that 1) the photolyzed ligand cannot migrate out of the protein matrix into the solvent, and hence only geminate rebinding can occur; 2) the protein sample is structurally heterogeneous and therefore the activation barrier for ligand recombination is not discrete; and 3) after photolysis the protein cannot relax to the deoxy structure, and ligand binding occurs in a "ligated-like" conformation. Low-temperature x-ray diffraction studies on photolyzed myoglobin crystals under steady illumination confirm this picture (Schlichting et al., 1994). Above ~160 K the protein undergoes large-scale structural fluctuations, and the B state produced by photolysis can either move back to A or give rise to the S state. In addition, ligand photolysis induces a change in conformation toward the deoxy structure such that geminate rebinding requires a higher activation energy, inasmuch as it is accompanied by a return to the ligand bound configuration. At the structural level, the increased activation barrier, observed above ~160 K for the B → A process, has been attributed to a larger displacement of the iron from the heme plane in the high-temperature compared to the low-temperature photoproduct, made possible by the increased mobility of the protein (Agmon and Hopfield, 1983; Nienhaus et al., 1994; Srajer et al., 1988; Steinbach et al., 1991). Various attempts have been made to develop a model capable of describing ligand binding kinetics above the glass transition temperature, taking into account conformational relaxation. Agmon and Hopfield (1983) where the first to deal with this problem, by using a single diffusion constant to describe the relaxation of a conformational coordinate, taken to be perpendicular to the reaction coordinate. A big drawback of this approach is that a discrete diffusion process is inconsistent with the observation that protein relaxation is not exponential in time (Frauenfelder et al., 1990). Later attempts to improve the agreement with experimental findings (Agmon et al., 1994; Agmon and Rabinovich, 1992) have only partially improved the situation. In the approach followed by Steinbach et al. (1991), the distribution of activation barriers, which accounts for the nonexponential ligand binding below ~160 K, is assumed to shift to higher energies with stretched exponential kinetics, according to what is observed experimentally (Frauenfelder et al., 1990). To simplify the formalism, they considered the shape of the distribution to be unaffected by the relaxation process, an approximation that is clearly tenable in some cases (Lambright et al., 1993; Steinbach et al., 1991) but is not generally applicable. The group of Wolynes has approached the general problem of coupling a chemical reaction with a slowly fluctuating environment, using a dominant path for its relaxation (Wang and Wolynes, 1993, 1994). This approach has been successfully applied to describing the kinetics of CO binding to sperm whale Mb (Panchenko et al., 1995).

Recent time-resolved x-ray crystallography investigations have provided some hints on the dynamics involved in the structural relaxation process that accompany laser photolysis of carbon monoxymyoglobin at room temperature (Srajer et al., 1996). The electron density maps show that 4 ns after photolysis, the iron atom is already fully displaced from the heme plane, whereas other structural rearrangements, particularly of the F-helix, extend into the microsecond time range.

To gain more insight into the functional implications of protein dynamics and their thermal evolution, we have undertaken a flash photolysis investigation of the kinetics of geminate CO binding to the monomeric erythrocruorin component III extracted from the larvae of the insect *Chironomus thummi-thummi* (CTT-Hb-III). We have chosen this protein because it is unique in many respects. Its ligand affinity increases with pH (Gersonde et al., 1986), and a pronounced conformational change accompanies the transition from the low-affinity to the high-affinity state (Gersonde et al., 1976; La Mar et al., 1978; Peyton et al., 1991), such that soaking crystals of CTT-Hb-III obtained at acidic pH in alkaline buffer causes them to crack (Steigemann and Weber, 1979). Thus, despite its relatively simple monomeric structure, CTT-Hb-III undergoes pH-induced conformational transitions and is therefore particularly well suited to pinpointing possible relationships between protein dynamics and functional complexity. Based on NMR data (La Mar et al., 1978; Peyton et al., 1991; Ribbing et al., 1978; Zhang et al., 1996), it has also been proposed that in CTT-Hb-III the heme can assume two distinct orientations, because of a rotation by π rad of the tetrapyrrole along the α-γ methine axis. The orientational transition is proton induced and occurs in the same pH region where the conformational changes responsible for the Bohr effect take place. Finally, according to the crystallographic data reported by Steigemann and Weber (1979), CTT-Hb-III displays the typical Mb folding, but in its ferrous ligand-free state, the heme iron barely protrudes from the porphyrin plane, being displaced by only ~17 pm, compared to ~35 pm in deoxy SW-Mb or ~58 pm in the α human Hb-A subunits (Perutz et al., 1987). This unusually small displacement of the heme iron in deoxy CTT-Hb-III contradicts the low-frequency resonance Raman spectrum reported by Kerr et al., (Kerr et al., 1985) for the same derivative, characterized by a sharp and intense line at 220 cm^{-1} and therefore indicative of a definitely larger out-of-plane position of the metal. Flash photolysis studies of CTT-Hb-III over broad temperature ranges are expected to provide new insight into this important issue.

MATERIALS AND METHODS

Sample preparation and instrumentation

Larvae of *Chironomus thummi-thummi* were kept at ~180 K in batches of ~50 g and were thawed only immediately before starting the erythrocruorin purification procedure, performed according to the method of Kleinschmidt et al. (1989). The purified protein in the CO-bound form and

in 1 mM potassium phosphate (pH 7) was concentrated by ultrafiltration to ~2 mM, rapidly frozen (Di Iorio, 1981), and kept in liquid nitrogen until immediately before use. The amount of protein necessary for a flash photolysis measurement was thawed and added to a mixture of glycerol and aqueous buffer previously saturated with pure CO at 20°C. Final concentrations were ~80 μM protein, 0.1 M K-borate (pH 9), or K-phosphate (pH 7) and 75% glycerol. Trace amounts of Na-dithionite were added to ensure the total absence of oxygen and of ferric erythrocruorin. The solution was immediately transferred anaerobically to a gold-plated copper cell previously purged with CO and equipped with polycarbonate windows. The cell was mounted on the cryostat, and kinetic measurements were performed by monitoring the absorbance changes induced by a single 10-ns photolyzing laser pulse at 436 nm, as described previously (Di Iorio et al., 1991, 1993). To allow complete relaxation to the ligated state, the recording of each kinetic trace below ~160 K was followed by a heating of the sample to at least 160 K and recooling to the desired temperature before performing the next measurement. We have collected two sets of data, both at pH 7 and at pH 9, taking 5–10 traces at each temperature. Time courses recorded under identical conditions were averaged and reduced for further analysis, as previously described (Di Iorio et al., 1991). Light absorption spectra of the samples in the cryostat cell were taken at the beginning and at the end of each measurement section.

Data analysis

To account for the nonexponential nature of the CO recombination kinetics at low temperatures, we used a model based on a distribution of activation enthalpies and a discrete value of the preexponential k_0. Accordingly, the absorbance change $\Delta A(t,T)$ at time t after photolysis and for a time course recorded at the absolute temperature T is given by

$$\Delta A(t, T) = \Delta A(t = 0, T) \cdot \int_0^\infty dH \cdot g(H) \cdot \exp\left[-\frac{T}{T_0} k_0 \cdot \exp\left(-\frac{H}{RT} \right) \cdot t \right] \quad (2)$$

where T_0 is arbitrarily taken to be 100 K (Doster et al., 1982). Being the numerical inversion of Eq. 2, an unstable procedure (McWirther and Pike, 1978), the $g(H)$ was parameterized by using the following modification of the model proposed by Young and Bowne (1984):

$$g(H) = H^{\Psi \cdot H_{peak}} \cdot \exp(-\Psi \cdot H) \quad (3)$$

and numerically normalized to unity area. Compared to the original model of Young and Bowne (1984), this approach reduces the number of parameters to only two without affecting the quality of the fittings (Boffi et al., 1994; Cupane et al., 1993; Di Iorio et al., 1991).

Global nonlinear least-squares fittings were done in the ΔA space according to the method of Marquardt (1963), weighting each experimental point on the basis of its reciprocal variance, computed from the experimental standard deviation in transmittance (Bevington, 1969, pp. 56–64). The numerical integration of Eq. 2 was done by the Romberg method to an accuracy of 10^{-5} ΔA units. Convergence was considered to be reached when the reduced global χ^2 changed by less than 10^{-4} between two successive iterations. The minimum model to be used for the analysis of the traces was decided on the basis of visual examination of the fittings and of an F-test (Bevington, 1969, pp. 195–202). After convergence the χ^2 hypersurface was scanned around the minimum for each parameter independently, and the upper and lower confidence limits were determined by the intersection points of the resulting curve with the 67% confidence line. This procedure is necessary when dealing with models involving enthalpy distributions, because the uncertainties in the values of the parameters obtained from the diagonal elements of the inverted curvature matrix (Bevington, 1969, pp. 242–245) are not realistic. Indeed, very often asymmetrical 67% confidence limits are obtained, implying that the parabolic expansion of the χ^2 hypersurface, on which the curvature matrix approach is based, is not tenable.

RESULTS

Up to 220 K only geminate CO binding is observed after photolysis of carbonyl-CTT-Hb-III, and the kinetic traces are well described by a single process with a discrete preexponential and a distributed activation enthalpy (Eqs. 2 and 3). Between 230 K and 280 K, a sum of one distributed and one discrete process (Eqs. 3 and 4) is needed, whereas at 290 K and 300 K a sum of two exponentials (Eq. 5) accounts well for the observed time courses of CO recombination:

$$\Delta A(t, T) = \Delta A(t = 0, T) \cdot \left\{ \begin{array}{l} f_g \cdot \int_0^\infty dH \cdot g(H) \cdot \exp\left[-\frac{T}{T_0} k_{0_g} \cdot \exp\left(-\frac{H_g}{RT} \right) \cdot t \right] + \\ f_s \cdot \exp\left[-\frac{T}{T_0} k_{0_s} \cdot \exp\left(-\frac{H_s}{RT} \right) \cdot t \right] \end{array} \right\} \quad (4)$$

$$\Delta A(t, T) = \Delta A(t = 0, T) \cdot \left\{ \begin{array}{l} f_g \cdot \exp\left[-\frac{T}{T_0} k_{0_g} \cdot \exp\left(-\frac{H_g}{RT} \right) \cdot t \right] \\ + f_s \cdot \exp\left[-\frac{T}{T_0} k_{0_s} \cdot \exp\left(-\frac{H_s}{RT} \right) \cdot t \right] \end{array} \right\} \quad (5)$$

In Eqs. 4 and 5, subscripts g and s refer, respectively, to the geminate and solvent processes, and the $f_g + f_s = 1$ boundary condition is applied. Examples of the results obtained are given in Fig. 1, where we report the experimental time courses at representative temperatures, along with the corresponding fitted traces.

The global fitting programs used for our data analysis allow high flexibility concerning the linking schemes between the fitting parameters. Thus we can determine which values need to be varied independently for each experimental trace and which do not. At both pH values investigated, the best compromise between total number of parameters whose values are left independently variable during the fittings and the resulting reduced global χ^2 is obtained with the linking scheme reported in Table 1.

The thermal evolution of the activation energy distributions for geminate ligand binding displays the same overall features at both pHs, but differs in the details. This appears from Figs. 2 and 3, where we report the temperature dependence of the apparent activation enthalpy distributions $g(H)$, as they result from our analysis approach. In Fig. 2 one can identify three regions: one below ~50 K, in which the apparent peak activation barrier drops very rapidly with decreasing temperature; a second one between ~50 K and ~170 K, where a small but significant drift of the H_{peak} is observed; and a third above ~170 K, characterized by a sharp thermal transition of the activation enthalpy. The

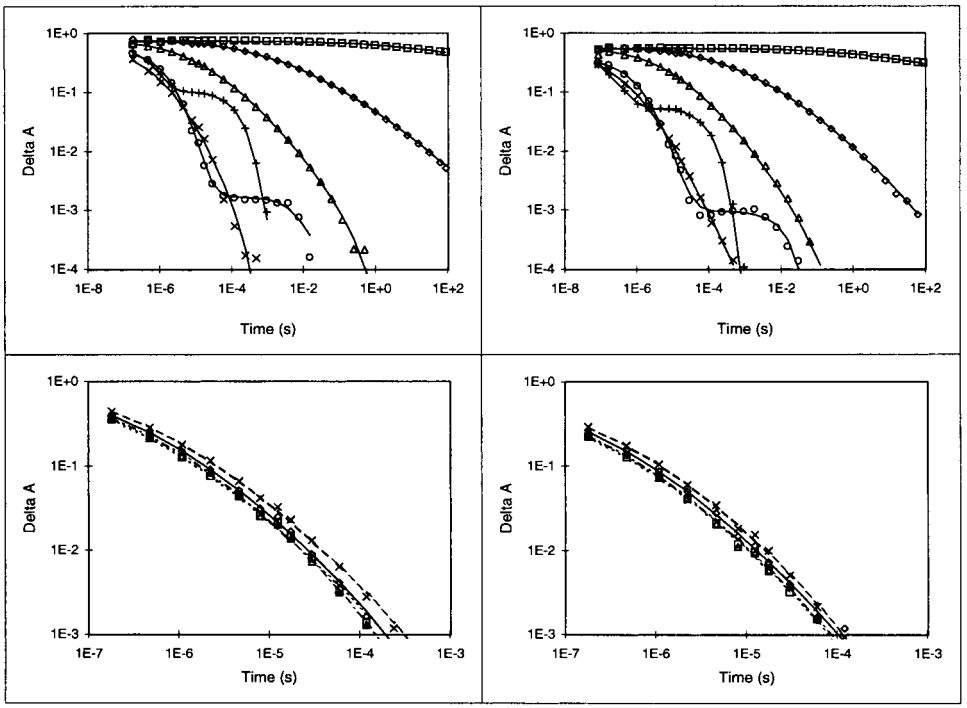

FIGURE 1 Time courses for CO recombination to CTT-Hb-III in 75% glycerol and 0.1 M phosphate, pH 7 (*left*), and 0.1 M borate pH 9 (*right*). Symbols refer to the experimental data and lines to the results of global fitting to Eqs. 4 (240 K), 5 (280 K), or 2 (all other traces). The top panels depict traces at 40 K (□), 80 K (◇), 120 K (△), 220 K (×), 240 K (○) and 280 K (+), and the bottom panels show time courses at 180 K (×, – – –), 190 K (◇, ——), 200 K (△, – · –), and 210 K (□, ·····).

latter phenomenon is reflected by a very modest temperature dependence of the geminate CO binding time courses between ~180 K and ~210 K, as shown in the lower panels of Fig. 1. The significance of the H_{peak} increase between 50 K and 170 K is illustrated in Fig. 3 (*lower panels*), where we report several $g(H)$ distributions in this temperature range, and in Fig. 4, which shows a comparison of experimental data recorded at 60 K, 80 K, and 100 K, with traces computed using the H_{peak} values that best describe the 40 K kinetics. It is quite obvious that a global fitting with the same H_{peak} value for all low-temperature traces cannot adequately account for the experimental results.

Up to 170 K the width of the $g(H)$ is not appreciably influenced by temperature, but this is no longer the case above ~170 K, where the distribution first broadens up to ~210 K, then becomes progressively narrower with increasing temperature, and eventually collapses to a line above 280 K (Fig. 3, *upper panel*).

The preexponential factor for geminate CO binding to CTT-Hb-III (derived from our analysis approach) is also pH dependent, being lower by one order of magnitude at pH 7 than at pH 9 (Table 2).

DISCUSSION

The CO binding kinetics of CTT-Hb-III are quite fast (Fig. 1). This reduces considerably the signal-to-noise ratio of the data, particularly in the temperature region just above the glass transition, such that the heuristic approach just described is the only practicable way for the analysis of the experimental time courses. Nevertheless, our formalism is capable of describing well the experimental results and allows the identification of several interesting features. We discuss the results of this analysis separately for the regions below and above the glass transition temperature. Whenever

TABLE 1 Linking scheme used for the global fitting of the CO binding kinetics to CTT-Hb-III

T (K)	$\Delta A(t = 0, T)$	f_g	H_{peak_g} or H_g	Ψ	log k_{o_g}	f_s	H_s	log k_{o_s}
40–170	V	—	V	L	L	—	—	—
180–210	V	—	V	V	L	—	—	—
220	V	V	V	V	L	—	—	—
230	V	V	V	V	L	C	F	L
240	V	V	V	V	L	C	V	L
250–280	V	V	V	V	L	C	V	L
290–300	V	V	V	—	L	C	V	L

V stands for variable, L for linked (viz., the same fitted value applies to the whole temperature range investigated), C for committed due to boundary conditions, and F fixed. Parameters' symbols are as defined in Eq. 4. At both pHs the 230 K traces are characterized by a very poor signal-to-noise ratio in the time region where the solvent process is observed. Therefore, the corresponding activation enthalpies were estimated from separate fittings of the data, limited to the relevant time region. The resulting values were used as constants (F) during the global analyses.

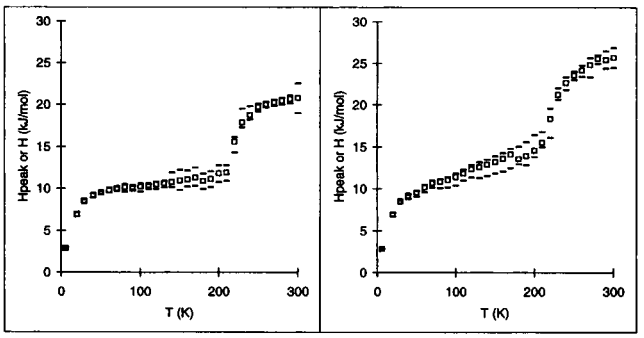

FIGURE 2 Temperature dependence of the apparent peak activation enthalpy for CO binding to CTT-Hb-III in 75% glycerol and 0.1 M phosphate, pH 7 (*left*), and 0.1 M borate, pH 9 (*right*). The bars above and below the symbols refer to the 67% confidence limits, computed as described in Materials and Methods.

particularly relevant, the limits of the model used are also discussed.

Kinetic behavior of CTT-Hb-III below 170 K

Despite the structural heterogeneity of CTT-Hb-III, arising from the silent mutation E6(57) Thr/Ile (Kleinschmidt et al., 1989), the low-temperature kinetics of CO binding to this protein, as obtained by monitoring in the Soret region, are well described by a single reaction step, characterized by relatively narrow $g(H)$ distributions at both pH 7 and pH 9. This contrasts with what is seen in analogous measurements on other proteins, whose low-temperature CO binding kinetics are accounted for by a single process with a broad $g(H)$, as in sperm whale Mb (Steinbach et al., 1991), reflecting the convolution of several underlying distributions (Di Iorio et al., 1991; Johnson et al., 1996; Prusakov et al., 1995), or require the use of complex models involving two or more kinetic components, as reported for various other systems (Boffi et al., 1994; Cupane et al., 1993; Di Iorio et al., 1991). Because the low-temperature $g(H)$ distributions for CO binding to CTT-Hb-III are quite narrow, relatively small changes produced by temperature on their peak position and/or shape can be easily detected. Figs. 2–4 show that H_{peak} is influenced by temperature changes well below 170 K and that our kinetic data are accurate enough to detect this relationship.

Tunneling through the activation barrier dominates at very low temperatures (Alberding et al., 1976a,b). Our model does not account for this phenomenon. Thus the H_{peak} values erroneously appear to be progressively lower, with decreasing temperature below ~50 K, and it would have been totally meaningless to plot the width of the corresponding $g(H)$ distributions in the top panel of Fig. 3.

The H_{peak} drift observed between ~50 K and ~170 K, where large-scale dynamics and tunneling can both be excluded, is a peculiarity that demands discussion. Based only on kinetic measurements probing electronic bands of the heme, we cannot decide with certainty if the observed

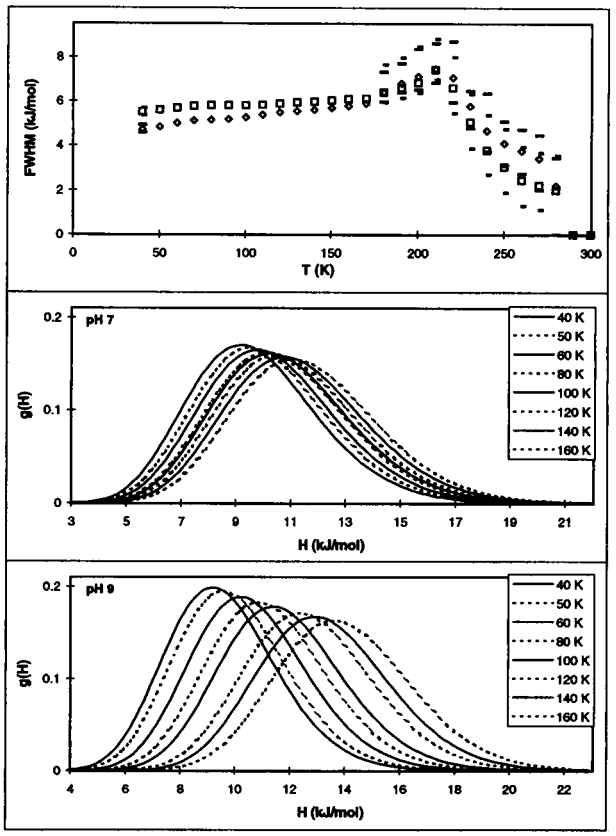

FIGURE 3 Thermal evolution of the $g(H)$ for CO binding to CTT-Hb-III in 75% glycerol and 0.1 M phosphate, pH 7 (*squares and narrow bars*), and 0.1 M borate, pH 9 (*diamonds and wide bars*), resulting from the analysis described in Materials and Methods. The top panel depicts the temperature dependence of the full width at half-maximum (FWHM) of the enthalpy distributions (symbols). The 67% confidence limits (*bars*) were computed from the confidence limits of the fitting parameter ψ. The 67% confidence limits given for the width at 40 K apply to the whole 40–170 K temperature range. The two lower panels show the thermal evolution of the $g(H)$ between 40 K and 160 K, respectively, at pH 7 (*middle*) and pH 9 (*lowest*).

phenomenon reflects a real increase of the enthalpic barrier for the relaxation of a single B to a single A state, or a change in the relative population of a discrete number of B states, as reported for sperm whale Mb (Johnson et al., 1996; Mourant et al., 1993, and references therein). However, based particularly on the pH 9 data, where the increase in H_{peak} with temperature is more pronounced, we favor the first hypothesis, because the thermal evolution of the $g(H)$ distributions depicted in the lower panels of Fig. 3 would imply the involvement of an unusually large number of such substates, each populated within a very narrow temperature window. In any case, the observed shift of the enthalpy distribution provides evidence for some kind of structural relaxation even below 170 K, in agreement with previous proposals based on MD simulations (Loncharich and Brooks, 1990) and transient and static optical spectroscopy studies (Cupane et al., 1993; Di Iorio et al., 1991). A plausible structural explanation for the H_{peak} shift is a

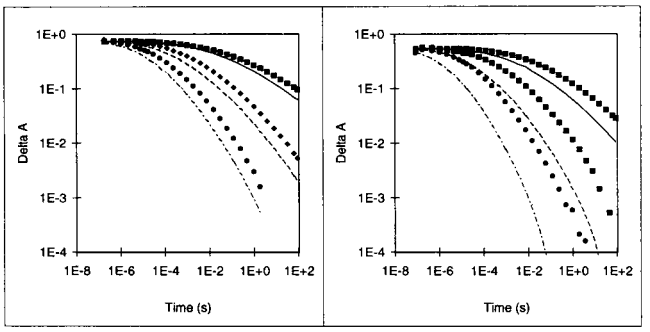

FIGURE 4 Comparison of the experimental time courses (*symbols*) for CO binding to CTT-Hb-III at three temperatures with traces (*lines*) computed using the H_{peak} value relative to the 40 K data. Curves corresponding to 60 K (■, ——), 80 K (◆, – – –), and 100 K (●, – · –) are shown.

change of the azimuthal angle ϕ, formed by the plane of the proximal histidine ring with the N1-Fe-N3 axis of the heme (Ahmed et al., 1991; Friedman et al., 1990; Gilch et al., 1993; Stavrov, 1993). In sperm whale and horse Mb this phenomenon is induced, below 160 K, by prolonged illumination of the carbonyl derivative (Nienhaus et al., 1994). In CTT-Hb-III the same structural transition could be thermally induced, but the currently available information forces us to remain at a purely speculative level in this respect. Furthermore, our data do not provide any valuable hint as to whether H_{peak} rises because of a continuous or a discrete structural relaxation. In the former case the transition would produce a shift in the $g(H)$ along the H axis without affecting its shape; in the latter the distribution should be narrower at the beginning and at the end of the transition and broader during the relaxation. The increase with temperature of the $g(H)$ width between ~40 K and ~170 K depicted in Fig. 3 would be indicative of a stepwise transition (Nienhaus et al., 1994). However, the onset of much larger structural fluctuations above ~170 K completely masks any further thermal evolution of the low-temperature $g(H)$ distribution. Furthermore, the width change between ~40 K and ~160 K depicted in Fig. 3 is biased by our fitting conditions, which force the parameter ψ to be temperature independent (Table 1).

CTT-Hb-III displays a pronounced Bohr effect, resulting from the interconversion between two conformational states (Gersonde et al., 1976; La Mar et al., 1978; Peyton et al., 1991; Steigemann and Weber, 1979). At the two pH values selected for our measurements, either one of the two configurations is dominating. The lower temperature dependence of H_{peak} at pH 7, compared to pH 9 (Fig. 2), suggests a higher susceptibility of the prosthetic group to local fluctuations in the high pH conformation of CTT-Hb-III. This is consistent with a higher preexponential for geminate CO binding at alkaline pH (Table 2), because an increased k_0 reflects a smaller heme pocket volume (Frauenfelder and Wolynes, 1985). During the preparation of our samples, the protein has not been subjected to a long enough incubation at the final pH of the measurements to allow heme reorientation. Therefore, we attribute the different low-temperature behavior of CTT-Hb-III at the two pHs to the conformational transition of the protein moiety and not to differences in heme orientation.

Kinetic behavior of CTT-Hb-III above 170 K

Just above 170 K the width of the enthalpy distribution for geminate CO rebinding to CTT-Hb-III, obtained from our fitting procedure, appears to increase up to ~210 K, where it reaches a maximum. Thereafter the $g(H)$ becomes progressively narrower, and at room temperature the kinetic process is exponential in time (Fig. 3). The apparent broadening of the $g(H)$ observed between ~170 K and ~220 K is

TABLE 2 Values of the fitting parameters obtained by global least-squares approximation of the CO binding kinetics to CTT-Hb-III

	pH 7			pH 9		
T (K)	H_{peak} (kJ/mol)	Ψ (mol/kJ)	log k_0/s	H_{peak} (kJ/mol)	Ψ (mol/kJ)	log k_0/s
	{9.40}	{1.79}	{10.04}	{9.30}	{2.35}	{10.73}
40	9.18	1.69	9.62	9.17	2.29	10.60
	{8.91}	{1.62}	{9.34}	{8.82}	{2.14}	{10.12}
	{9.96}			{9.78}		
50	9.51	L	L	9.55	L	L
	{9.26}			{9.05}		
	{12.11}			{14.25}		
160	11.10	L	L	13.63	L	L
	{10.22}			{12.10}		
	{22.54}			{27.86}		
300	20.79	∞	L	25.70	∞	L
	{18.99}			{23.47}		

Only the results relative to geminate CO binding at representative temperatures are given. In curly brackets we report the 67% confidence limits. L stands for linked value (see Table 1). Details about the fitting and error analysis procedures are given in Materials and Methods.

clearly an artifact introduced by the use of a single distribution model to describe the experimental data. In this temperature range protein molecules that bind the ligand, before any structural relaxation to the unligated conformation can take place, coexist with molecules that undergo the conformational transition before or while ligand binding occurs. Thus, in the simplest case, the $g(H)$ obtained from our fittings is a convolution of enthalpy distributions for the unrelaxed (lower H_{peak}) and relaxed (higher H_{peak}) system. A more complex formalism that models the structural relaxation accompanying ligand binding (Panchenko et al., 1995; Post et al., 1993; Steinbach et al., 1991) would certainly be more appropriate. Unfortunately, because of the poor signal-to-noise ratio of the traces in this critical temperature range, even fittings with a sum of two distributions are ill conditioned. Nevertheless, the apparent broadening of the single $g(H)$ used in our simple model between ~170 K and ~220 K gives an idea of the speed of relaxation phenomena in CTT-Hb-III and their thermal evolution. Most interesting is the progressive narrowing of the $g(H)$ above ~220 K, which leads to a complete collapse of the distribution at room temperature. Again, we are forced to propose only a phenomenological interpretation of our results because of the impossibility of treating the data with more quantitative models. However, our data unequivocally show that, above 280 K, the interconversion between conformational substates in CTT-Hb-III becomes faster than geminate CO rebinding. In this case the model proposed by Steinbach et al. (1991), where the structural relaxation is assumed to shift the $g(H)$ distribution derived from low-temperature kinetics toward higher enthalpy values without influencing its width, would have not been applicable. The room temperature collapse of the geminate CO-binding enthalpy distribution to a line is also indicative of a high structural flexibility of CTT-Hb-III. According to the proposal of Di Iorio et al. (1991), a high structural flexibility of CTT-Hb-III is also indicated by the comparatively narrow enthalpy distribution observed below ~170 K.

As mentioned in the Introduction, the crystallographic data available for CTT-Hb-III point to a very small displacement of the heme iron from the tetrapyrrol plane in its deoxy derivative. This feature, according to the structural relaxation models proposed in the literature (Agmon and Hopfield, 1983; Srajer et al., 1988; Steinbach et al., 1991), would predict a minimal (if any) increase of the activation barrier for geminate ligand binding to CTT-Hb-III above ~170 K. Our data show that this is not the case. The apparent peak activation enthalpy for geminate CO binding at 170 K is ~11.3 kJ mol^{-1} at pH 7 and ~14.1 kJ mol^{-1} at pH 9, whereas the enthalpy barrier for the same process at 300 K increases, respectively, to ~20.8 kJ mol^{-1} and ~25.7 kJ mol^{-1} (Fig. 2). Thus either the displacement from the heme plane in the deoxy derivative is larger than reported by Steigeman and Weber (1979), as Raman spectroscopy investigations would imply (Kerr et al., 1985), or other structural parameters, beside the position of the iron relative to the tetrapyrrol plane, must be considered to account for the increase in activation energy for geminate CO rebinding observed above ~170 K. A good candidate would be the tilt angle θ, formed by the proximal bond with the heme plane (Ahmed et al., 1991; Friedman et al., 1990; Gilch et al., 1993; Nienhaus et al., 1994; Stavrov, 1993).

Structural flexibility and functional complexity

To gain insight into a possible role of protein dynamics during evolution, we compare the behavior of CTT-Hb-III with that reported for the homodimeric hemoglobin of the mollusk *Scapharca inaequivalvis* (Scapharca Hb-I) (Boffi et al., 1994). CTT-Hb-III displays a considerable structural flexibility, and as already discussed, its reactivity is regulated by pH-induced conformational changes of the protein moiety (Gersonde et al., 1976, 1986; La Mar et al., 1978; Peyton et al., 1991), a sophisticated mechanism to fine-tune the functional properties of the molecule. On the other hand, Scapharca Hb-I has a high structural rigidity (Boffi et al., 1994; Ilari et al., 1995) and displays no sign of heterotropic modulation of its functional properties (Chiancone et al., 1981). Furthermore, it is well documented that homotropic interactions in this protein arise from a direct communication between the two hemes, mediated by structured water at the subunit interface (Royer et al., 1996) and with very limited involvement of the protein moiety (Chiancone et al., 1990, 1993; Pardanani et al., 1997). The opposite dynamic and functional behavior displayed by CTT-Hb-III and Scapharca Hb-I suggests a link between structural flexibility and complexity of the molecular mechanism used to modulate the reactivity of the active site, as also indicated, but not as clearly, by previous comparative investigations (Alberding et al., 1978; Bisig et al., 1995; Boffi et al., 1994; Cupane et al., 1993; Di Iorio et al., 1991, 1993; Dlott et al., 1983). Rigid proteins appear to be characterized by a low level of functional complexity, whereas a higher structural flexibility seems to accompany a more sophisticated functional regulation. We therefore propose an evolutionary role of protein dynamics, postulating that proteins with higher rigidity are generally preferred by nature to increase their stability against thermal denaturation, but higher degrees of structural flexibility are introduced in response to the demand for more complex functional behaviors.

CONCLUDING REMARKS

The kinetic data reported here are limited to a monitoring of CO recombination only in the Soret region of the electronic spectrum and to an analysis based on a heuristic model. Even though necessarily qualitative, this study points to two crucial differences between the dynamic behavior of CTT-Hb-III and that of myoglobins, particularly of sperm whale Mb, which is taken, mainly for historical reasons, to be the reference system: 1) A temperature dependence of the activation barrier for geminate CO binding below the glass transition temperature and 2) a collapse to a single expo-

nential of the barrier distribution for the same ligand-binding step at room temperature. Both phenomena are consistent with a higher structural flexibility of CTT-Hb-III compared to that of myoglobins. Furthermore, the very small iron displacement from the heme plane reported by Steigeman and Weber for the deoxy derivative of CTT-Hb-III (Steigemann and Weber, 1979) is questioned by our results and by those of Kerr et al. (1985). Both of the explanations that we have proposed for the peculiar kinetic behavior of CTT-Hb-III and the discrepancy with the crystallographic data will be the subject of a specific infrared and Raman spectroscopy investigation.

The authors are indebted to K. W. Winterhalter for his interest in this work and precious suggestions, and to A. Lehman for technical support.

This work was supported by the ETH Zurich (0-20-690-93 and special credit 03586/41-1080.5). Financial support to IT by the Kontakt-Gruppe für Forschungsfragen of the Basle Chemical Industries is kindly acknowledged.

REFERENCES

Abadan, Y., E. Y. T. Chien, K. Chu, C. D. Eng, G. U. Nienhaus, and S. G. Sligar. 1995. Ligand binding to heme-proteins. V. Light-induced relaxation in proximal mutants L89I and H97F of carbon monoxymyoglobin. *Biophys. J.* 68:2497–2504.

Agmon, N., W. Doster, and F. Post. 1994. The transition from inhomogeneous to homogeneous kinetics in CO binding to myoglobin. *Biophys. J.* 66:1612–1622.

Agmon, N., and J. J. Hopfield. 1983. CO binding to heme proteins: a model for barrier height distributions and slow conformational changes. *J. Chem. Phys.* 79:2042–2053.

Agmon, N., and S. Rabinovich. 1992. Diffusive dynamics on potential energy surfaces: nonequilibrium CO binding to heme proteins. *J. Chem. Phys.* 97:7271–7286.

Ahmed, A. M., B. F. Campbell, D. Caruso, M. R. Chance, M. D. Chavez, S. H. Courtney, J. M. Friedman, I. E. T. Iben, M. R. Ondrias, and M. Yang. 1991. Evidence for proximal control of ligand specificity in hemeproteins: absorption and Raman studies of cryogenically trapped photoproducts of ligand bound myoglobins. *Chem. Phys.* 158:329–351.

Alberding, N., R. H. Austin, K. W. Beeson, S. S. Chan, L. Eisenstein, H. Frauenfelder, and T. M. Nordlund. 1976a. Tunneling in ligand binding to heme proteins. *Science.* 192:1002–1004.

Alberding, N., R. H. Austin, S. S. Chan, L. Eisenstein, H. Frauenfelder, I. C. Gunsalus, and T. M. Nordlund. 1976b. Dynamics of carbon monoxide binding to protoheme. *J. Chem. Phys.* 65:4701–4711.

Alberding, N., S. S. Chan, L. Eisenstein, H. Frauenfelder, D. Good, I. C. Gunsalus, T. M. Nordlund, M. F. Perutz, A. H. Reynolds, and L. B. Sorensen. 1978. Binding of carbon monoxide to isolated hemoglobin chains. *Biochemistry.* 17:43–51.

Andreani, C., A. Filabozzi, F. Menzinger, A. Desideri, A. Deriu, and D. Di Cola. 1995. Dynamics of hydrogen atoms in superoxide dismutase by quasielastic neutron scattering. *Biophys. J.* 68:2519–2523.

Ansari, A., J. Berendzen, S. F. Bowne, H. Frauenfelder, I. E. Iben, T. B. Sauke, E. Shyamsunder, and R. D. Young. 1985. Protein states and proteinquakes. *Proc. Natl. Acad. Sci. USA.* 82:5000–5004.

Ansari, A., J. Berendzen, D. Braunstein, B. R. Cowen, H. Frauenfelder, M. K. Hong, I. E. T. Iben, J. B. Johnson, P. Ormos, T. B. Sauke, R. Scholl, A. Schulte, P. J. Steinbach, J. Vittitov, and R. D. Young. 1987. Rebinding and relaxation in the myoglobin pocket. *Biophys. Chem.* 26:337–355.

Antonini, E., and M. Brunori. 1971. Hemoglobin and Myoglobin in Their Reactions with Ligands. North-Holland Publishing Company, Amsterdam, London.

Austin, R. H., K. Beeson, L. Eisenstein, H. Frauenfelder, I. C. Gunsalus, and V. P. Marshall. 1973. Dynamics of carbon monoxide binding by heme proteins. *Science.* 181:541–543.

Bevington, P. R. 1969. Data Reduction and Error Analysis for the Physical Sciences. McGraw-Hill Book Company, New York.

Bisig, D. A., E. E. Di Iorio, K. Diederichs, K. H. Winterhalter, and K. Piontek. 1995. Crystal structure of Asian elephant (*Elephas maximus*) cyano-metmyoglobin at 1.78-Å resolution. Phe29(B10) accounts for its unusual ligand binding properties. *J. Biol. Chem.* 270:20754–20762.

Boffi, A., D. Verzili, E. Chiancone, L. Cordone, A. Cupane, M. Leone, V. Militello, E. Vitrano, W. Yu, and E. E. Di Iorio. 1994. Stereodynamic properties of the cooperative homodimeric *Scapharca inaequivalvis* hemoglobin studied through optical absorption spectroscopy and ligand rebinding kinetics. *Biophys. J.* 67:1713–1723.

Bosenbeck, M. R., R. Schweitzer-Stenner, and W. Dreybrodt. 1992. pH induced conformational changes of the Fe^{2+}-N(HisF8) linkage in deoxyhemoglobin trout IV detected by the Raman active Fe^{2+}-N(HisF8) stretching mode. *Biophys. J.* 61:31–41.

Braunstein, D. P., K. Chu, K. D. Egeberg, H. Frauenfelder, J. R. Mourant, G. U. Nienhaus, P. Ormos, S. G. Sligar, B. A. Springer, and R. D. Young. 1993. Ligand binding to heme proteins. III. FTIR studies of His-E7 and Val-E11 mutants of carbon monoxymyoglobin. *Biophys. J.* 65:2447–54.

Causgrove, T. P., and R. B. Dyer. 1993. Protein response to photodissociation of CO from carbon monoxymyoglobin probed by time-resolved infrared spectroscopy of the amide-I band. *Biochemistry.* 32: 11985–11991.

Chiancone, E., R. Elber, W. E. Royer, Jr., R. Regan, and Q. H. Gibson. 1993. Ligand binding and conformation change in the dimeric hemoglobin of the clam *Scapharca inaequivalvis. J. Biol. Chem.* 268: 5711–5718.

Chiancone, E., P. Vecchini, D. Verzili, F. Ascoli, and E. Antonini. 1981. Dimeric and tetrameric hemoglobins from the mollusc *Scapharca inaequivalvis.* Structural and functional properties. *J. Mol. Biol.* 152: 577–592.

Chiancone, E., D. Verzili, A. Boffi, W. E. Royer, and W. A. Hendrickson. 1990. A cooperative hemoglobin with directly communicating hemes—the *Scapharca inaequivalvis* homodimer. *Biophys. Chem.* 37:287–292.

Cupane, A., M. Leone, V. Militello, M. E. Stroppolo, F. Polticelli, and A. Desideri. 1994. Low temperature optical spectroscopy of native and azide reacted bovine Cu, Yn superoxide dismutase. A structural dynamics study. *Biochemistry.* 33:15103–15109.

Cupane, A., M. Leone, E. Vitrano, L. Cordone, U. R. Hiltpold, K. H. Winterhalter, W. M. Yu, and E. E. Di Iorio. 1993. Structure-dynamics-function relationships in asian elephant (*Elephas maximus*) myoglobin. An optical spectroscopy and flash-photolysis study on functionally important motions. *Biophys. J.* 65:2461–2472.

Di Iorio, E. E. 1981. Preparation of derivatives of ferrous and ferric hemoglobin. *Methods Enzymol.* 76:57–72.

Di Iorio, E. E., U. R. Hiltpold, D. Filipovic, K. H. Winterhalter, E. Gratton, E. Vitrano, A. Cupane, M. Leone, and L. Cordone. 1991. Protein dynamics. Comparative investigation on heme-proteins with different physiological roles. *Biophys. J.* 59:742–754.

Di Iorio, E. E., W. Yu, C. Calonder, K. H. Winterhalter, G. De Sanctis, G. Falcioni, F. Ascoli, B. Giardina, and M. Brunori. 1993. Protein dynamics in minimyoglobin: is the central core of myoglobin the conformational domain? *Proc. Natl. Acad. Sci. USA.* 90:2025–2029.

Di Pace, A., A. Cupane, M. Leone, E. Vitrano, and L. Cordone. 1992. Protein dynamics. Vibrational coupling, spectral broadening mechanisms, and anharmonicity effects in carbonmonoxy heme proteins studied by the temperature dependence of the Soret band lineshape. *Biophys. J.* 63:475–484.

Dlott, D. D., H. Frauenfelder, P. Langer, H. Roder, and E. E. Di Iorio. 1983. Nanosecond flash photolysis study of carbon monoxide binding to the beta chain of hemoglobin Zurich [beta 63(E7)His leads to Arg]. *Proc. Natl. Acad. Sci. USA.* 80:6239–6243.

Doster, W., D. Beece, S. F. Bowne, E. E. Di Iorio, L. Eisenstein, H. Frauenfelder, L. Reinisch, E. Shyamsunder, K. H. Winterhalter, and K. T. Yue. 1982. Control and pH dependence of ligand binding to heme proteins. *Biochemistry.* 21:4831–4839.

Doster, W., S. F. Bowne, H. Frauenfelder, L. Reinisch, and E. Shyamsunder. 1987. Recombination of carbon monoxide to ferrous horseradish peroxidase types A and C. *J. Mol. Biol.* 194:299–312.

Doster, W., S. Cusack, and W. Petry. 1989. Dynamical transition of myoglobin revealed by inelastic neutron scattering. *Nature.* 337: 754–756.

Doster, W. S., S. Cusack, and W. Petry. 1990. Dynamical instability of liquid like motions in globular proteins observed by inelastic neutron scattering. *Phys. Rev. Lett.* 65:1080–1083.

Frauenfelder, H., N. Alberding, A. Ansari, D. Braunstein, B. R. Cowen, M. K. Hong, I. E. T. Iben, J. B. Johnson, S. Luck, J. R. Mourant, P. Ormos, L. Reinisch, R. Scholl, A. Shulte, E. Shyamsunder, L. B. Sorensen, P. J. Steinbach, X. Aihua, R. D. Young, and K. T. Yue. 1990. Proteins and pressure. *J. Phys. Chem.* 94:1024–1037.

Frauenfelder, H., and P. G. Wolynes. 1985. Rate theories and puzzles of heme protein kinetics. *Science.* 229:337–345.

Friedman, J. M., B. F. Campbel, and R. W. Noble. 1990. A possible new control mechanism suggested by resonance Raman spectra from a deep ocean fish hemoglobin. *Biophys. Chem.* 37:43–59.

Friedman, J. M., D. L. Rousseau, M. R. Ondrias, and R. A. Stepnoski. 1982. Transient Raman study of hemoglobin: structural dependence of the iron-histidine linkage. *Science.* 218:1244–1246.

Gersonde, K., L. Noll, H. T. Gaud, and S. J. Gill. 1976. A calorimetric study of the CO Bohr effect of monomeric haemoglobins. *Eur. J. Biochem.* 62:577–582.

Gersonde, K., H. Twilfer, and M. Overkamp. 1986. Bohr effect in monomeric insect haemoglobins controlled by O_2 off-rate and modulated by heam-rotational disorder. *Eur. J. Biochem.* 157:393–404.

Gilch, H., R. Schweitzer-Stenner, and W. Dreybrodt. 1993. Structural heterogeneity of the Fe^{2+}-N(His^{F8}) bond in various hemoglobin and myoglobin derivatives probed by the Raman-active iron histidine stretching mode. *Biophys. J.* 65:1470–1485.

Glumoff, T. 1991. On the structure and properties of lignine perxidase: a biochemical and crystallographic study. PhD thesis. Laboratory of Biochemistry. Eidgenössische Technische Hochschule, Zurich, Switzerland.

Hong, M. K., D. Braunstein, B. R. Cowen, H. Frauenfelder, I. E. T. Iben, J. R. Mourant, P. Ormos, R. Scholl, A. Schulte, P. J. Steinbach, A. H. Xie, and R. D. Young. 1990. Conformational substates and motions in myoglobin. External influences on structure and dynamics. *Biophys. J.* 58:429–436.

Ilari, A., A. Boffi, and E. Chiancone. 1995. Rigidity of the heme pocket in the cooperative Scapharca hemoglobin homodimer and relation to the direct communication between hemes. *Arch. Biochem. Biophys.* 316: 378–384.

Ivanov, D., J. T. Sage, M. Keim, J. R. Powell, S. A. Asher, and P. M. Champion. 1994. Determination of CO orientation in myoglobin by single crystal infrared linear dichroism. *J. Am. Chem. Soc.* 116: 4139–4140.

Johnson, J. B., D. C. Lamb, H. Frauenfelder, J. D. Muller, B. McMahon, G. U. Nienhaus, and R. D. Young. 1996. Ligand binding to heme proteins. 6. Interconversion of taxonomic substates in carbonmonoxymyoglobin. *Biophys. J.* 71:1563–1573.

Kerr, E. A., N. T. Yu, K. Gersonde, D. W. Parish, and K. Smith. 1985. Iron-histidine stretching vibration in the deoxy state of insect hemoglobins with different O_2 affinities and Bohr effects. *J. Biol. Chem.* 260: 12665–12669.

Kleinschmidt, T., H. G. Keyl, and G. Braunitzer. 1989. Comparison of insect hemoglobins (erythrocruorins) from *Chironomus thummi-thummi* and *Chironomus thummi-piger* (diptera). The primary structure of the monomeric hemoglobin CTP III. *Biol. Chem. Hoppe-Seyler.* 370: 838–845.

Krupyanskii, Y. F., V. I. Goldanskii, G. U. Nienhaus, and F. Parak. 1990. Dynamics of protein-water systems revealed by Rayleigh scattering of Mössbauer radiation (RSMR). *Hyperfine Interactions.* 53:59–74.

La Mar, G. N., M. Overkamp, H. Sick, and K. Gersonde. 1978. Proton nuclear magnetic resonance hyperfine shifts as indicators of tertiary structural changes accompanying the Bohr effect in monomeric insect hemoglobins. *Biochemistry.* 17:352–361.

Lambright, D. G., S. Balasubramanian, and S. G. Boxer. 1993. Dynamics of protein relaxation in site-specific mutants of human myoglobin. *Biochemistry.* 32:10116–10124.

Loncharich, R. J., and B. R. Brooks. 1990. Temperature dependence of dynamics of hydrated myoglobin. Comparison of force field calculations with neutron scattering data. *J. Mol. Biol.* 215:439–455.

Marquardt, D. W. 1963. An algorithm for least squares estimation of nonlinear parameters. *J. Soc. Ind. Appl. Math.* 11:431–441.

McWirther, J. G., and E. R. Pike. 1978. On the numerical inversion of Laplace transform and Fredholm integral equations of the first kind. *J. Phys. A Math. Gen.* 11:1297–1745.

Morikis, D., P. M. Champion, B. A. Springer, K. D. Egebey, and S. G. Sligar. 1990. Resonance Raman studies of iron spin and axial coordination in distal pocket mutants of ferric myoglobin. *J. Biol. Chem.* 265:12143–12145.

Morikis, D., P. M. Champion, B. A. Springer, and S. G. Sligar. 1989. Resonance Raman investigations of site-directed mutants of myoglobin: effects of distal histidine replacement. *Biochemistry.* 28:4791–4800.

Mourant, J. R., D. P. Braunstein, K. Chu, H. Frauenfelder, G. U. Nienhaus, P. Ormos, and R. D. Young. 1993. Ligand binding to heme proteins. II. Transitions in the heme pocket of myoglobin. *Biophys. J.* 65: 1496–1507.

Nienhaus, G. U., J. R. Mourant, K. Chu, and H. Frauenfelder. 1994. Ligand binding to heme proteins: the effect of light on ligand binding in myoglobin. *Biochemistry.* 33:13413–13430.

Panchenko, A. R., J. Wang, G. U. Nienhaus, and P. G. Wolynes. 1995. Analysis of ligand binding to heme proteins using a fluctuation path description. *J. Phys. Chem.* 99:9278–9282.

Parak, F. 1989. Structural distributions, fluctuations and conformational changes in proteins investigated by Mössbauer spectroscopy and X-ray structure analysis. *NATO Adv. Sci. Inst. Ser. A Life Sci.* 178:197–221.

Pardanani, A., Q. H. Gibson, G. Colotti, and W. E. Royer. 1997. Mutation of residue Phe(97) to Leu disrupts the central allosteric pathway in Scapharca dimeric hemoglobin. *J. Biol. Chem.* 272:13171–13179.

Perutz, M. F., G. Fermi, B. Luisi, B. Shaanan, and R. C. Liddington. 1987. Stereochemistry of cooperative mechanisms in hemoglobin. *Acc. Chem. Res.* 20:309–321.

Peyton, D. H., G. N. La Mar, S. Ramaprasad, S. W. Unger, S. Sankar, and K. Gersonde. 1991. Proton nuclear magnetic resonance study of the solution distal histidine orientation in monomeric *Chironomus thummi-thummi* cyanomet hemoglobins. Dynamic stability of the heme pocket as monitored by labile proton exchange. *J. Mol. Biol.* 221:1015–1026.

Post, F., W. Doster, G. Karvounis, and M. Settles. 1993. Structural relaxation and nonexponential kinetics of CO-binding to horse myoglobin. Multiple flash photolysis experiments. *Biophys. J.* 64:1833–1842.

Prusakov, V. E., J. Steyer, and F. G. Parak. 1995. Mössbauer spectroscopy on nonequilibrium states of myoglobin. A study on r-t transition. *Biophys. J.* 68:2524–2530.

Ribbing, W., D. Krümpelmann, and H. Rüterjans. 1978. Isomeric incorporation of the haem group into two monomeric haemoglobins of *Chironomus thummi-thummi. FEBS Lett.* 92:105–108.

Richter, C., and E. E. Di Iorio. 1991. Analysis of the membrane-bound cytochrome P-450 system by the flash-photolysis technique. *In* Frontiers in Biotransformation. Akademie Verlag, Berlin. 72–93.

Royer, W. E., A. Pardanani, Q. H. Gibson, E. S. Peterson, and J. M. Friedman. 1996. Ordered water molecules as key allosteric mediators in a cooperative dimeric hemoglobin. *Proc. Natl. Acad. Sci. USA.* 93: 14526–14531.

Schlichting, I., J. Berendzen, G. N. Phillips, Jr., and R. M. Sweet. 1994. Crystal structure of photolysed carbonmonoxy-myoglobin. *Nature.* 371: 808–812.

Schomacker, K. T., and P. M. Champion. 1986. Investigations of spectral broadening mechanisms in biomolecules: cytochrome *c*. *J. Chem. Phys.* 84:5314–5325.

Schweitzer-Stenner, R., U. Dannemann, and W. Dreybrodt. 1992. Investigation of the heme distortions and heme-protein coupling in the isolated subunits of oxygenated human hemoglobin by resonance Raman dispersion spectroscopy. *Biochemistry.* 31:694–702.

Spiro, T. G. 1988. Biological Applications of Raman Spectroscopy. Wiley and Sons, New York.

Srajer, V., and P. M. Champion. 1991. Investigations of optical line shapes and kinetic hole burning in myoglobin. *Biochemistry.* 30:7390–7402.

Srajer, V., L. Reinisch, and P. M. Champion. 1988. Protein fluctuations, distributed coupling, and the binding of ligands to heme proteins. *J. Am. Chem. Soc.* 110:6656–6670.

Srajer, V., T. Y. Teng, T. Ursby, C. Pradervand, Z. Ren, S. Adachi, W. Schildkamp, D. Bourgeois, M. Wulff, and K. Moffat. 1996. Photolysis of the carbon monoxide complex of myoglobin: nanosecond time-resolved crystallography. *Science.* 274:1726–1729.

Stavrov, S. S. 1993. The effect of iron displacement out of the porphyrin plane on the resonance Raman spectra of heme proteins and iron porphyrins. *Biophys. J.* 65:1942–1950.

Steigemann, W., and E. S. Weber. 1979. Structure of erythrocruorin in different ligand states refined at 1.4 Å resolution. *J. Mol. Biol.* 127: 309–338.

Steinbach, P. J., A. Ansari, J. Berendzen, D. Braunstein, K. Chu, B. R. Cowen, D. Ehrenstein, H. Frauenfelder, J. B. Johnson, D. C. Lamb, S. Luck, J. R. Mourant, G. U. Nienhaus, P. Ormos, R. Philipp, R. Schopp, A. Xie, and R. D. Young. 1991. Ligand binding to heme proteins: connection between dynamics and function. *Biochemistry.* 30: 3988–4001.

Stetzkowski, F., R. Banerjee, M. C. Marden, D. K. Beece, S. F. Bowne, W. Doster, L. Eisenstein, H. Frauenfelder, L. Reinisch, E. Shyamsunder, and C. Jung. 1985. Dynamics of dioxygen and carbon monoxide binding to soybean leghemoglobin. *J. Biol. Chem.* 260:8803–8809.

Wang, J., and P. Wolynes. 1993. Passage through fluctuating geometrical bottlenecks. The general gaussian fluctuating case. *Chem. Phys. Lett.* 212:427–433.

Wang, J., and P. Wolynes. 1994. Survival paths for reaction dynamics in fluctuating environments. *Chem. Phys.* 180:141–156.

Young, R. D., and S. F. Bowne. 1984. Conformational substates and barrier height distributions in ligand binding to heme proteins. *J. Chem. Phys.* 81:3730–3737.

Zhang, W., G. N. LaMar, and K. Gersonde. 1996. Solution H-1-NMR structure of the heme cavity in the low-affinity state for the allosteric monomeric cyano-met hemoglobins from *Chironomus thummi thummi*—comparison to the crystal structure. *Eur. J. Biochem.* 237: 841–853.